Research Paper
Computational Methods for Differential Equations
http://cmde.tabrizu.ac.ir
Vol. 14, No. 1, 2026, pp. 316-336
DOI:10.22034/cmde.2024.57475.2405

Numerical solution of linear and nonlinear Schrödinger equations via the shifted Chebyshev collocation method

Nidhi Prabhakar and Seema Sharma*
Department of Mathematics and Statistics, Gurukul Kangri (Deemed to be University), Haridwar, Uttarakhand.

Abstract

The present study focuses on numerical solutions of linear and nonlinear Schr¨odinger equations subject to initial and boundary conditions employing the shifted Chebyshev spectral collocation method (SCSCM). In the solution procedure, unknown function and its space derivatives have been approximated employing shifted Chebyshev polynomials and their derivatives, respectively, together with Chebyshev-Gauss-Lobatto points. The present collocation method transforms the Schrödinger equation into a system of ordinary differential equations (ODEs). Thereafter, the obtained system has been solved employing the fourth-order Runge-Kutta scheme. To demonstrate the accuracy and efficiency of the present method, a comparison of the present numerical solutions of different examples of the Schrödinger equation with exact and approximate solutions available in the literature has been discussed. The SCSCM can be implemented to solve second and higher-order linear and nonlinear partial differential equations (PDEs) arising in physics, mechanics, and biophysics.

Keywords. Shifted Chebyshev polynomials, Spectral collocation method, Schrödinger equation, Runge-Kutta method.
2010 Mathematics Subject Classification. 65M70, 35G16, 35G31.

1. Introduction

The Schrödinger equation is a PDE that depicts the wave function of a quantum-mechanical system. Schrödinger equation is quantum analogous to Newton's law in classical physics. In order to make predictions and to understand quantum mechanical systems, the Schrödinger equation is essential, in the same way as Newton's law is important to predict the motion of a physical system with given initial conditions. This equation occurs in a variety of forms, including linear, nonlinear, time-dependent, and time-independent.

Consider the important nonlinear one-dimensional time-dependent Schrödinger equation [33] with cubic nonlinear term $|w|^2w$ defined as:

$$iw_t + \phi w_{xx} + \mu|w|^2w + \delta w = 0, \qquad t \in (0, T], \tag{1.1}$$

subject to initial condition

$$w(x, 0) = g(x), \qquad x \in [\alpha, \beta], \tag{1.2}$$

and dirichlet boundary conditions

$$w(\alpha, t) = f_0(t), \qquad w(\beta, t) = f_1(t), \tag{1.3}$$

where, $i = \sqrt{-1}, w(x, t)$ is a complex-valued function, T is final time, ϕ, μ, and δ are constant parameters. Equation (1.1) becomes linear for $\mu = 0$.

Numerous researchers over the past few decades have been working to solve linear and nonlinear PDEs like Schrödinger equation because of widespread use of these equations to describe natural phenomena, and it is still an active area of study currently. Analytical solutions of Schrödinger equations are usually extremely challenging and

Received: 10 July 2023; Accepted: 09 December 2024.
∗ Corresponding author. Email: seema@gkv.ac.in.

perhaps impossible. The initial condition also affects the solution of a time-dependent Schrödinger equation. For many generic initial conditions, the analytical solutions of the nonlinear Schrödinger equation are unknown. Various numerical techniques have been applied by researchers to solve the nonlinear Schrödinger equation with different types of initial and boundary conditions numerically because of the non-availability of its analytical solutions. It includes the spline collocation method [26], finite difference schemes (FDS) [9], quadratic B-spline finite element method [10], quartic spline finite difference method [30], split-step finite difference method [35], time-space pseudo-spectral method [12], Pade scheme [31], quintic B-spline finite element method [28], multi-quadrics (MQ) quasi-interpolation technique [14], Jacobi-Gauss-Lobatto collocation (J-GL-C) method [13], Haar wavelet collocation method (HWCM) [23], Legendre spectral element method [18], HWCM [24], hybrid method involving finite difference and Haar wavelets [3], Haar wavelet finite difference hybrid method [19], Crank-Nicolson method [16].

Numerical solutions of nonlinear PDEs [5, 21, 22, 25] are important from numerical perspectives and researchers have adopted various numerical methods for obtaining numerical solutions for such equations. During the last few decades, the spectral collocation method, one of the most effective methods, has been used to obtain the numerical solutions of different nonlinear PDEs with boundary and initial conditions [6, 7, 11, 38]. This powerful method has been chosen because of its higher convergence rate [8, 34] and this method produces excellent accuracy even with a small number of collocation points. The formulation of Chebyshev polynomials based spectral collocation method is simple, requires minimum human effort and nevertheless maintains accuracy for the numerical solutions. Therefore, various researchers have applied Chebyshev collocation methods (CCM) for solving various types of differential equations numerically. Sharma et al. [29] employed CCM to study the frequencies of vibrations of polar orthotropic annular plates. Zarebnia and Jalili [37] obtained numerical solutions of different nonlinear PDEs, such as Huxley, Burger's Huxley, generalized Burger's Fisher and Fisher's equations by employing Chebyshev spectral collocation method. Ashrafi et al. [4] solved Gardner and Huxley equation using the spectral collocation method. Jaiswal et al. [15] applied Shifted Chebyshev polynomials operational matrix method for solving nonlinear PDEs like Burgers, Fisher, Huxley, Burgers-Huxley, and Burgers-Fisher equation. Aghdam et al. [2] employed CCM of the third kind for solving space fractional diffusion equation. Mesgarani et al. [20] obtained numerical solutions of the fractional Black-Scholes equation employing CCM involving second-kind shifted Chebyshev polynomials. Aghdam et al. [1] solved the space fractional diffusion equation by employing CCM of the fourth kind. CCM of the fourth kind has been employed by Safdari et al. [27] for obtaining a numerical solution of space time fractional advection diffusion equation. Wang et al. [36] solved Emden-Fowler equation using Picard iteration and CCM.

Although much work has been done for solving Schrödinger equation but to the best of the authors knowledge, SCSCM has not yet been applied to solve Schrödinger equation. In the present paper, SCSCM has been applied with fourth-order Runge-Kutta scheme to obtain an approximate solution of the linear and nonlinear Schrödinger equation. SCSCM employs Chebyshev polynomials for collocation purposes, which have the minimax property among polynomial family with the property of orthogonality. Because of this property, the SCSCM is a significant technique for obtaining highly accurate approximate solutions of Schrödinger equation among other existing numerical techniques. In the solution procedure, Chebyshev polynomials have been applied to approximate the unknown functions and their space derivatives in Schrödinger equation. These approximations give rise to a system of nonlinear ODEs. Also, the selection of collocation points is crucial for the convergence and efficiency of the present method. Here, Chebyshev-Gauss-Lobatto points have been chosen to be collocation points. Thereafter, Runge-Kutta scheme of order four is applied to solve the resulting system of nonlinear ODEs. The solutions of linear and nonlinear Schrödinger equations are complex-valued functions. The present method has been employed for seven examples of linear and nonlinear Schrödinger equations and L_∞ and L_2 error norms in numerical solutions for different numbers of collocation points N have been presented to validate the accuracy and efficiency of the present method. The obtained numerical results of these examples are compared with exact and approximate solutions obtained by other numerical techniques and are shown in graphical and tabular form. It is observed that error norms get decreased by increasing the value of N and highly accurate solutions are obtained mostly for N=10. Further, the error norms for the present method have been compared with error norms for other numerical methods such as HWCM, MQ quasi-interpolation technique and J-GL-C method. In comparison to these approaches, the present method provides better accuracy for a smaller number of collocation points. Thus, it consumes less processing time and computer memory for obtaining higher accuracies in

numerical solutions. It is revealed from Example 5.7 that both the error norms are smaller for $\triangle$t=0.0001 and they reduce to the order of 10^{-15} taking $N = 10$. Therefore, the present method is an efficient, accurate, effective and useful method to obtain the approximate solutions of linear and nonlinear Schrödinger equations. It will be helpful for the researchers and analysts who are engaged in numerical studies of modelling of different linear and nonlinear physical and engineering problems. The SCSCM can be extended for solving coupled and higher-dimensional linear and nonlinear Schrödinger equations.

This paper is organised as follows. Basic preliminaries of Chebyshev polynomials and shifted Chebyshev polynomials are given in section 2. Application of SCSCM for the solution of Schrödinger equation is described in section 3. Section 4 presents some examples of Schrödinger equation and their numerical solutions. At last, the conclusions are discussed in section 5.

2. Chebyshev polynomials preliminaries

2.1. **Chebyshev polynomials of the first kind.** The Chebyshev polynomials $T_m(p)$ on $[-1, 1]$ are given as

$$T_m(p) = cos(mcos^{-1}p). \tag{2.1}$$

Alternatively, these Chebyshev polynomials can also be obtained by using the following recurrence relation

$$T_m(p) = 2pT_{m-1}(p) - T_{m-2}(p), \qquad m = 2, 3, \ldots, \tag{2.2}$$

with $T_0(p) = 1, T_1(p) = p$.

The Chebyshev polynomials are orthogonal and their inner products are given as

$$\langle T_m(p), T_n(p)\rangle = \int_{-1}^{1} \frac{T_m(p)T_n(p)}{\sqrt{1-p^2}}dp = \begin{cases} 0, & m \neq n, \\ \pi, & m = n = 0, \\ \pi/2, & m = n \neq 0. \end{cases} \tag{2.3}$$

where $\frac{1}{\sqrt{1-p^2}}$ is the weight function.

2.2. **Shifted Chebyshev polynomials of the first kind.** The Chebyshev polynomials $T_m(p)$ are defined on $[-1, 1]$. Chebyshev polynomials $T^*_m(x)$ can be used for a general interval $[\alpha, \beta]$ by transforming this interval to the applicability range $[-1, 1]$ using the transformation

$$p = \frac{2x - (\alpha + \beta)}{\beta - \alpha}. \tag{2.4}$$

Thus, shifted Chebyshev polynomials of the first kind, denoted by $T^*_m(x)$ are given by

$$T^*_m(x) = T_m\left(\frac{2x - (\alpha + \beta)}{\beta - \alpha}\right). \tag{2.5}$$

These polynomials can be constructed using the recurrence relation

$$T^*_m(x) = 2\left(\frac{2x - (\alpha + \beta)}{\beta - \alpha}\right)T^*_{m-1}(x) - T^*_{m-2}(x), \qquad m = 2, 3, \ldots. \tag{2.6}$$

with $T^*_0(x) = 1, T^*_1(x) = \frac{2x-(\alpha+\beta)}{\beta-\alpha}$.

These polynomials also satisfy the orthogonality condition and all the properties of the first kind Chebyshev polynomials.

2.3. **Derivative of shifted Chebyshev polynomials.** The first-order derivative of shifted Chebyshev polynomials is given by

$$T_m^{*\prime}(x) = 2m\gamma \sum_{j=0,\ (j+m)\ odd}^{m-1} a_j T_j^*(x), \tag{2.7}$$

where, $\gamma = \frac{2}{\beta-\alpha}$ and

$$a_j = \begin{cases} 1, & 1 \le j \le N-1, \\ \frac{1}{2}, & j = 0, N. \end{cases} \tag{2.8}$$

3. Solution of Schrödinger equation by shifted Chebyshev spectral collocation method

The Schrödinger Equation (1.1) can be rewritten as

$$w_t - i\phi w_{xx} - i\mu|w|^2 w - i\delta w = 0, \qquad t \in (0, T], \tag{3.1}$$

with initial condition

$$w(x, 0) = g(x), \qquad x \in [\alpha, \beta], \tag{3.2}$$

and dirichlet boundary conditions

$$w(\alpha, t) = f_0(t), \qquad w(\beta, t) = f_1(t). \tag{3.3}$$

To solve the Schrödinger Equation (3.1) with given conditions (3.2) and (3.3), approximate the solution function $w(x, t)$ using shifted Chebyshev polynomials as

$$w(x, t) = \sum_{m=0}^{N}{}'' c_m T_m^*(x). \tag{3.4}$$

where $T_m^*(x)$ indicates the m^{th} shifted Chebyshev polynomial of the first kind and coefficients c_m are given by [17]

$$c_m = \frac{2}{N} \sum_{k=0}^{N}{}'' T_m^*(x_k) w(x_k, t). \tag{3.5}$$

Here, the addition of the first and end terms has been halved and denoted by summation with double quotes. The Chebyshev-Gauss-Lobatto collocation points x_k are defined as

$$x_k = \frac{1}{2}\left((\alpha+\beta) - (\beta-\alpha)cos\left(\frac{\pi k}{N}\right)\right), \qquad k = 0, 1, \ldots, N. \tag{3.6}$$

By differentiating Equation (3.4), the derivative $w_x(x, t)$ is approximated as

$$w_x(x, t) = \sum_{m=0}^{N}{}'' c_m T_m^{*\prime}(x) = \sum_{k=0}^{N}{}'' \left(\frac{2}{N} \sum_{m=0}^{N}{}'' T_m^{*\prime}(x) T_m^*(x_k)\right) w(x_k, t).$$

Now, the derivative $w_x(x, t)$at collocation point x_j is given by

$$w_x(x_j, t) = \sum_{k=0}^{N}{}'' \left(\frac{2}{N} \sum_{m=0}^{N}{}'' T_m^{*\prime}(x_j) T_m^*(x_k)\right) w(x_k, t) = \sum_{k=0}^{N} [P_x]_{jk} w(x_k, t), \tag{3.7}$$

where

$$[P_x]_{jk} = \frac{2a_j}{M} \sum_{m=0}^{N}{}'' T_m^{*\prime}(x_j) T_m^*(x_k), \qquad j, k = 0, 1, \ldots, N,$$

and $T_m^{*\prime}(x_j)$ and a_j are given by Equations (2.7) and (2.8), respectively.

Further, by differentiating Equation (3.7), the second order derivative at collocation point x_j, $w_{xx}(x_j,t)$ can be approximated as

$$\begin{aligned} w_{xx}(x_j,t) &= \sum_{k=0}^{N}[P_x]_{jk}w_x(x_k,t) \\ &= \sum_{k=0}^{N}[P_x]_{jk}\left(\sum_{l=0}^{N}[P_x]_{kl}w(x_l,t)\right) \\ &= \sum_{l=0}^{N}\left(\sum_{k=0}^{N}[P_x]_{jk}[P_x]_{kl}\right)w(x_l,t) \\ &= \sum_{l=0}^{N}[Q_x]_{jl}w(x_l,t), \end{aligned} \tag{3.8}$$

where $[Q_x]_{jl} = \sum_{k=0}^{N}[P_x]_{jk}[P_x]_{kl}$, $j,l = 0,1,\ldots,N$.

Now, by using boundary conditions (3.3), Equation (3.8) can be rewritten as

$$w_{xx}(x_j,t) = D_j(t) + \sum_{l=1}^{N-1}[Q_x]_{jl}w(x_l,t), \tag{3.9}$$

where $D_j(t) = [Q_x]_{j0}f_0(t) + [Q_x]_{jN}f_1(t)$.

Now, discretizing Equation (3.1) at internal collocation points $x_j; j = 1,2,\ldots,N-1$, it becomes

$$w_t(x_j,t) - i\phi w_{xx}(x_j,t) - i\mu|w(x_j,t)|^2w(x_j,t) - i\delta w(x_j,t) = 0, \qquad j = 1,2,\ldots,N-1. \tag{3.10}$$

Substituting expression (3.9) into Equation (3.10) and denoting $w(x_j,t)$ and $w_t(x_j,t)$ by $w_j(t)$ and $\dot{w}_j(t)$, respectively, leads to

$$\dot{w}_j(t) - i\phi\sum_{l=1}^{N-1}[Q_x]_{jl}w_l(t) - i\phi D_j(t) - i\mu|w_j(t)|^2w_j(t) - i\delta w_j(t) = 0, \qquad j = 1,2,\ldots,N-1, \tag{3.11}$$

along with the initial conditions

$$w_j(0) = w(x_j,0) = g(x_j), \quad j = 1,2,\ldots,N-1. \tag{3.12}$$

The system of ODEs (3.11) and initial conditions (3.12) can be expressed as

$$\begin{cases} \dot{w}(t) = \Psi(t,w(t)), \\ \text{and} \\ w(0) = w_0, \end{cases} \tag{3.13}$$

where,

$$\begin{aligned} w(t) &= [w_1(t), w_2(t), \ldots, w_{N-1}(t)]^T, \\ \dot{w}(t) &= [\dot{w}_1(t), \dot{w}_2(t), \ldots, \dot{w}_{N-1}(t)]^T, \\ w_0 &= [w_1(0), w_2(0), \ldots, w_{N-1}(0)]^T, \\ \Psi(t,w(t)) &= [\Psi_1(t,w(t)), \Psi_2(t,w(t)), \ldots, \Psi_{N-1}(t,w(t))]^T, \end{aligned}$$

and

$$\Psi_j(t,w(t)) = i\phi\sum_{l=1}^{N-1}[Q_x]_{jl}w_l(t) + i\phi D_j(t) + i\mu|w_j(t)|^2w_j(t) + i\delta w_j(t), \qquad j = 1,2,\ldots,N-1.$$

The system of Equations (3.13) is a system of first-order simultaneous ODEs. The solution of this system at $(i+1)^{th}$ time level $w(t_{i+1})$, when the solution at i^{th} time level $w(t_i)$ is known, can be obtained using fourth-order Runge-Kutta

scheme. This is an explicit scheme, which provides very accurate solutions. The solution $w(t_{i+1})$ of the system of ODEs (3.13) employing fourth-order Runge-Kutta scheme is given as

$$w(t_{i+1}) = w(t_i) + \frac{\Delta t}{6}[\Psi(t_i, w(t_i)) + 2\Psi\left(t_i + \frac{\Delta t}{2}, w^{(1)}\right) + 2\Psi\left(t_i + \frac{\Delta t}{2}, w^{(2)}\right) + \Psi(t_i + \Delta t, w^{(3)})], \tag{3.14}$$

where

$$w^{(1)} = w(t_i) + \frac{1}{2}\Delta t\Psi(t_i, w(t_i)),$$
$$w^{(2)} = w(t_i) + \frac{1}{2}\Delta t\Psi\left(t_i + \frac{\Delta t}{2}, w^{(1)}\right),$$
$$w^{(3)} = w(t_i) + \Delta t\Psi\left(t_i + \frac{\Delta t}{2}, w^{(2)}\right).$$

3.1. **Algorithm for Numerical Computation.** The algorithm for the shifted Chebyshev spectral collocation method is as follows:
Input: Declare N (No. of collocation points), T (final time), and $\triangle$t (step length).
Step 1: Compute collocation points.
Step 2: Compute shifted Chebyshev polynomials.
Step 3: Compute derivatives of shifted Chebyshev polynomials.
Step 4: Compute first-order and second-order derivatives of the function in terms of shifted Chebyshev polynomials and their derivatives.
Step 5: Discretize Schrödinger equation at collocation points.
Step 6: Substitute the second-order derivative of the unknown function in discretized Schrödinger equation.
Step 7: Formulate the system of ODEs.
Step 8: Solve the system of ODEs using the fourth-order Runge-Kutta scheme.
Output: The approximate solution $w(x, t)$ of Schrödinger equation is obtained.

4. Convergence analysis

In order to examine the convergence of SCSCM, the following convergence theorems are discussed.

Theorem 4.1. *The polynomials $2^{-(2m-1)}T_m^*(x)$ have the smallest norm among all m^{th} degree monic polynomials defined on the interval $[\alpha, \beta]$ i.e.,*

$$\|2^{-(2m-1)}T_m^*(x)\| = 2^{-(2m-1)}.$$

Proof. It can be proved following Chebyshev's theorem (See ref. [32]). □

Theorem 4.2. *If $w(x) \in L^2[a, b]$ is approximated in the form of a series of shifted Chebyshev polynomials. Then this series is strongly convergent.*

Proof. Let $w(x)$ be approximated in the form of a series of shifted Chebyshev polynomials $T_m^*(x)$ as

$$w(x) = \sum_{m=0}^{\infty} c_m T_m^*(x), \tag{4.1}$$

where,

$$T_m^*(x) = a_m((x-\alpha)(\beta-x))^{\frac{1}{2}}\frac{d^m}{dx^m}((x-\alpha)(\beta-x))^{m-\frac{1}{2}}. \tag{4.2}$$

The polynomials $T_m^*(x)$ are orthogonal w.r.t. the weight function

$$W(x) = ((x-\alpha)(\beta-x))^{-\frac{1}{2}}.$$

In Equation (4.1), the coefficients c_m are given by

$$c_m = \frac{\int_\alpha^\beta ((x-\alpha)(\beta-x))^{-\frac{1}{2}} w(x) T_m^*(x) dx}{\int_\alpha^\beta ((x-\alpha)(\beta-x))^{-\frac{1}{2}} T_m^*(x) T_m^*(x) dx}, \tag{4.3}$$

Substituting value of $T_m^*(x)$ from Equation (4.2) and integrating the numerator and denominator, we have

$$c_m = \frac{\int_\alpha^\beta ((x-\alpha)(\beta-x))^{m-\frac{1}{2}} w^{(m)}(x) dx}{m!\gamma_m \int_\alpha^\beta ((x-\alpha)(\beta-x))^{m-\frac{1}{2}} dx} = \frac{\int_\alpha^\beta W^m(x) w^{(m)}(x) dx}{m!\gamma_m \int_\alpha^\beta W^m(x) dx}, \tag{4.4}$$

where $\gamma_m = 2^{2m-1}$.

The value of the coefficient c_m is not more than a weighted mean with a non-negative weight function, therefore

$$c_m = \frac{w^{(m)}(\varphi)}{m!\gamma_m}, \qquad (\alpha \le \varphi \le \beta). \tag{4.5}$$

Now, writing Equation (4.1) as

$$w(x) = \sum_{m=0}^{N-1} c_m T_m^*(x) + E_N, \tag{4.6}$$

where,

$$E_N = \sum_{m=N}^{\infty} c_m T_m^*(x). \tag{4.7}$$

Now, $\sup_{\alpha \le x \le \beta} |T_m^*(x)| = 1$. Therefore, using Chebyshev truncation theorem, the bound on error is as

$$|E_N| \le \sum_{m=N}^{\infty} |c_m| \approx |c_N|. \tag{4.8}$$

Now, substitution of Equation (4.5) in Equation (4.8) yields

$$|E_N| \le \left| \frac{w^{(N)}(\varphi)}{(N)!\gamma_N} \right| = \left| \frac{w^{(N)}(\varphi)}{(N)!2^{2N-1}} \right|, \tag{4.9}$$

which shows that, $|E_N| \to 0$ as $N \to \infty$. Therefore, the accuracy in approximation using shifted Chebyshev polynomials gets improved as the value of N is increased. This shows that the series for $w(x)$ is strongly convergent. □

5. Numerical Examples

To demonstrate the accuracy, applicability and efficiency of the SCSCM, seven examples of linear and nonlinear Schrödinger equations are considered. "MATLAB R2015a" software has been used for numerical simulation on the laptop with a 1.30 GHz Intel Core i5 processor, 16GB RAM and a 64-bit operating system. Approximate solutions obtained by the present method are compared with solutions obtained by other methods given in literature and exact solutions. The solutions $w(x,t)$ of linear and nonlinear Schrödinger equations are complex-valued functions. Therefore, to verify the accuracy of SCSCM, the maximum absolute error norm L_∞ and L_2 error norm have been calculated using the following expressions

TABLE 1. L_∞ and L_2 error norms in approximate solutions of Example 5.1 at $t = 1$ taking $\Delta t = 0.001$.

N	$L_\infty(R(w))$	$L_\infty(I(w))$	$L_\infty(w)$	$L_2(R(w))$	$L_2(I(w))$	$L_2(w)$	CPU time (Seconds)
4	1.6249e-04	7.3766e-04	7.5535e-04	2.2980e-04	1.0432e-03	1.0682e-03	12.6
6	2.0265e-06	5.5469e-07	2.0271e-06	2.8759e-06	7.8744e-07	2.9818e-06	15.4
8	3.3057e-09	2.7962e-09	4.3297e-09	5.8447e-09	5.4788e-09	8.0111e-09	18.0
10	1.4285e-09	1.6898e-10	1.4384e-09	2.0551e-09	2.6274e-10	2.0718e-09	20.5

$$
\begin{aligned}
L_\infty(R(w)) &= \max_i |real(w_i^{exact}) - real(w_i)|,\\
L_\infty(I(w)) &= \max_i |imaginary(w_i^{exact}) - imaginary(w_i)|,\\
L_\infty(w) &= \max_i |w_i^{exact} - w_i|,\\
L_2(R(w)) &= \sqrt{\sum_{i=1}^{N} |real(w_i^{exact}) - real(w_i)|^2},\\
L_2(I(w)) &= \sqrt{\sum_{i=1}^{N} |imaginary(w_i^{exact}) - imaginary(w_i)|^2},\\
L_2(w) &= \sqrt{\sum_{i=1}^{N} |w_i^{exact} - w_i|^2},
\end{aligned}
$$

where, w_i^{exact} and w_i represent the exact and approximate solutions of Schrödinger equation at collocation points x_i.

Example 5.1. Consider linear diffusion form of Schrödinger equation taking $\phi = -1, \mu = 0$ and $\delta = 0$, i.e.

$$iw_t - w_{xx} = 0,$$

subject to Dirichlet boundary conditions

$$w(\alpha, t) = e^{it} sin(\alpha), \quad w(\beta, t) = e^{it} sin(\beta),$$

and initial condition

$$w(x, 0) = sin(x).$$

The exact solution is given by

$$w(x, t) = e^{it} sin(x).$$

The numerical solutions are depicted in tabular and graphical form for the domain $[\alpha, \beta] = [-1, 1]$. Table 1 shows error norms and CPU time for obtaining the solutions at $t = 1$ taking $\Delta t = 0.001$ and different numbers of collocation points N. It is found that the errors decrease by increasing the value of N. Further, the error norms reduce to order 10^{-9} for $N = 10$. Table 2 shows the comparison of L_∞ error norms in approximate solutions by the present method and existing solutions by HWCM [3] for different values of t taking $\Delta t = 0.001$. It is seen that in the case of HWCM, the error is of order 10^{-5} for $N = 32$, whereas, for the present method, it is of order 10^{-9} fixing $N = 10$. This shows the efficiency as well as accuracy of the SCSCM for the linear Schrödinger equation. The real parts of approximate and exact solutions have been depicted in Figure 1, while Figure 2 presents the imaginary parts of exact and approximate solutions of Example 5.1. The graphs of real and imaginary parts of exact and approximate solutions are almost the same, which demonstrates the accuracy of the present method.

TABLE 2. Comparison of L_∞ error norms in approximate solutions of Example 5.1 taking $\Delta t = 0.001$.

t	$L_\infty(R(w))$		$L_\infty(I(w))$		$L_\infty(w)$	
	HWCM ($N = 32$)	Present Method ($N = 10$)	HWCM ($N = 32$)	Present Method ($N = 10$)	HWCM ($N = 32$)	Present Method ($N = 10$)
1	2.670e-05	1.429e-09	6.011e-05	1.690e-10	6.578 e-05	1.438e-09
2	1.766e-05	2.427e-10	3.018e-05	2.205e-09	3.431 e-05	2.218e-09
4	4.698e-05	3.690e-10	3.105e-05	1.345e-09	5.632 e-05	1.395e-09
6	3.632e-05	5.232e-10	4.901 e-05	1.075e-09	6.100 e-05	1.196e-09
8	3.975e-05	1.111e-10	2.896 e-05	1.874e-09	4.919 e-05	1.878e-09
10	1.095e-05	7.118e-10	2.522 e-05	3.374e-10	2.708 e-05	7.878e-10

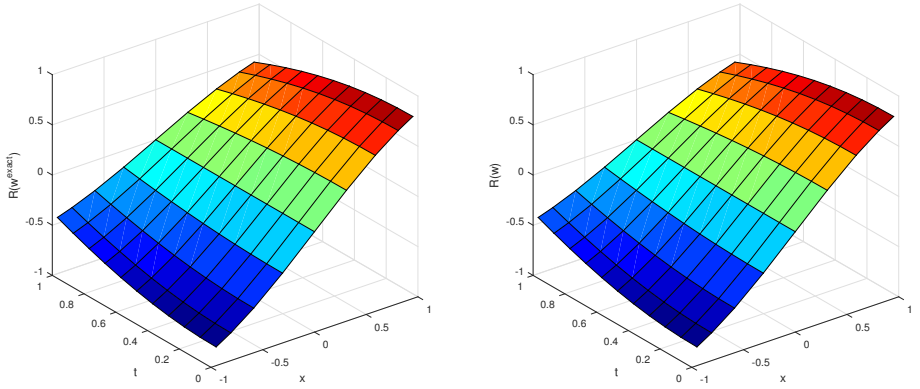

FIGURE 1. The real parts of exact and approximate solutions of Example 5.1 for $N = 10$.

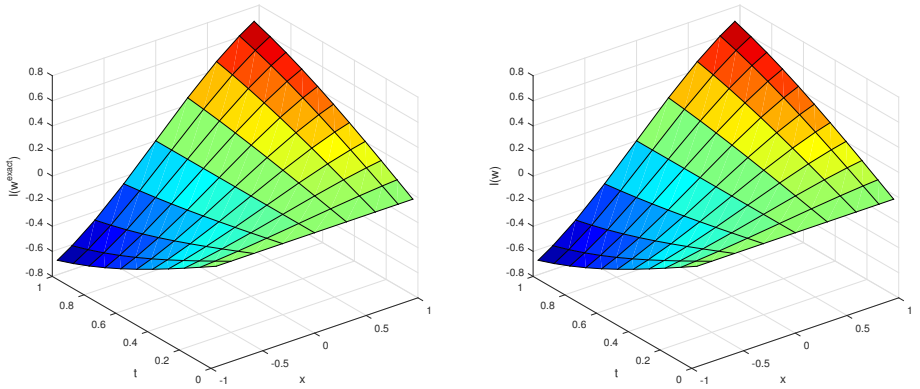

FIGURE 2. The imaginary parts of exact and approximate solutions of Example 5.1 for $N = 10$.

TABLE 3. L_∞ and L_2 error norms in approximate solutions of Example 5.2 taking different values of N and $\Delta t = 0.001$.

N	$L_\infty(R(w))$	$L_\infty(I(w))$	$L_\infty(w)$	$L_2(R(w))$	$L_2(I(w))$	$L_2(w)$	CPU time (Seconds)
2	7.7094e-02	5.4671e-03	7.7288e-02	7.7094e-02	5.4671e-03	7.7288e-02	8.0
4	6.8733e-04	1.1642e-04	6.9712e-04	8.2278e-04	8.3271e-04	1.2825e-04	10.6
6	7.0289e-07	1.2094e-07	7.0430e-07	1.1378e-06	1.4107e-07	1.1465e-06	13.9
8	1.6648e-09	1.4016e-09	2.1762e-09	2.0897e-09	2.7022e-09	3.4159e-09	17.3
10	1.1697e-10	4.8213e-10	4.9612e-10	1.8348e-10	6.8986e-10	7.1384e-10	20.8

TABLE 4. L_∞ and L_2 error norms in approximate solutions of Example 5.2 taking $N = 10$ and $\Delta t = 0.001$.

t	$L_\infty(R(w))$	$L_\infty(I(w))$	$L_\infty(w)$	$L_2(R(w))$	$L_2(I(w))$	$L_2(w)$
1	1.1697e-10	4.8213e-10	4.9612e-10	1.8348e-10	6.8986e-10	7.1384e-10
2	7.3427e-10	4.7906e-10	8.7672e-10	1.0640e-09	6.9519e-10	1.2710e-09
4	8.1581e-10	1.0251e-09	1.3101e-09	1.1841e-09	1.4851e-09	1.8993e-09
6	9.8081e-10	7.9837e-10	1.2647e-09	1.4205e-09	1.1601e-09	1.8340e-09
8	4.3350e-10	7.8667e-10	8.9820e-10	6.3282e-10	1.1388e-09	1.3028e-09
10	5.7780e-10	1.1235e-10	5.8862e-10	8.3661e-10	1.6059e-10	8.5189e-10

Example 5.2. Consider linear diffusion form of Schrödinger Equation (1.1), where $\phi = -1, \mu = 0$ and $\delta = 0$

$$iw_t - w_{xx} = 0,$$

subject to Dirichlet boundary conditions

$$w(\alpha, t) = e^{it}cos(\alpha), \qquad w(\beta, t) = e^{it}cos(\beta),$$

and initial condition

$$w(x, 0) = cos(x).$$

The exact solution is given by

$$w(x, t) = e^{it}cos(x).$$

The numerical solutions obtained by the present method are shown in Tables 3-5 and Figures 3 and 4 for the domain $[\alpha, \beta] = [-1, 1]$. Table 3 presents error norms and CPU time for obtaining approximate solutions of the linear Schrödinger equation at $t = 1$ by taking different values of N and $\Delta t = 0.001$. It is observed that the approximate solutions converge by increasing the value of N and the error norms reduce to order 10^{-10} for $N = 10$. Table 4 exhibits L_∞ and L_2 error norms in solutions obtained by the present method for distinct values of t taking $N = 10$ and $\Delta t = 0.001$. Table 5 shows the comparison of L_∞ error norms in solutions at $t = 1$ by the present method and HWCM [3]. It is observed that in comparison to HWCM, the present method provides better accuracy in approximate solutions for a smaller number of collocation points. The real and imaginary parts of exact and approximate solutions for various values of x and t have been depicted graphically in Figures 3 and 4.

TABLE 5. Comparison of L_∞ error norms in approximate solutions at $t = 1$ of Example 5.2 taking $\Delta t = 0.001$.

Error norm	HWCM(N=32)	Present Method(N=10)
$L_\infty(R(w))$	8.56e-05	1.17e-10
$L_\infty(I(w))$	5.38e-04	4.82e-10
$L_\infty(w)$	5.45e-04	4.96e-10

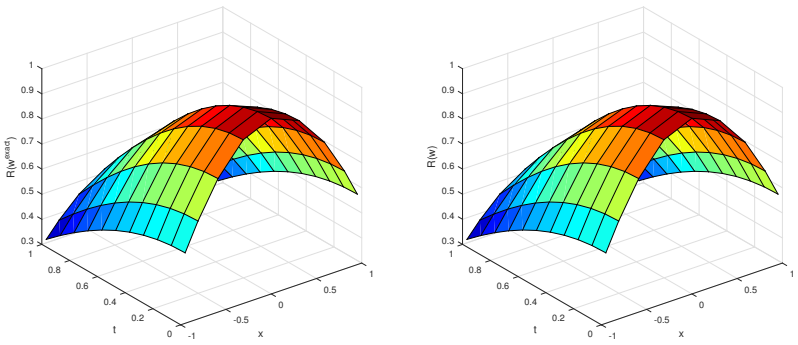

FIGURE 3. The real parts of exact and approximate solutions of Example 5.2 for $N = 10$.

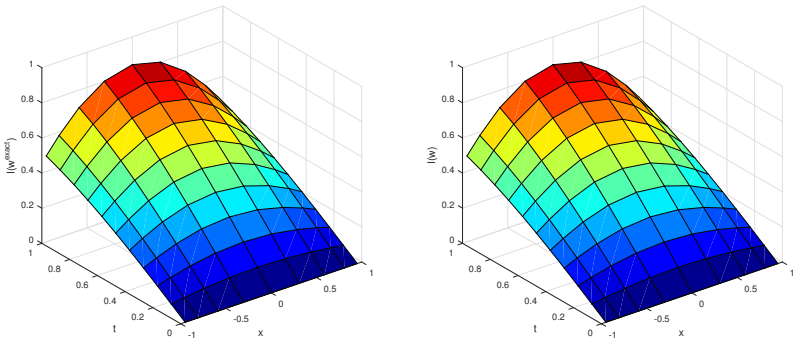

FIGURE 4. The imaginary parts of exact and approximate solutions of Example 5.2 for $N = 10$.

Example 5.3. The linear reaction-diffusion form of Equation (1.1) with variable coefficients by taking $\phi = 1, \mu = 0$ and $\delta = 1 - \frac{2}{x^2}$ is given as

$$iw_t + w_{xx} + (1 - \frac{2}{x^2})w = 0,$$

subject to Dirichlet boundary conditions

$$w(\alpha, t) = \alpha^2 e^{it}, \quad w(\beta, t) = \beta^2 e^{it},$$

and initial condition

$$w(x, 0) = x^2.$$

TABLE 6. Comparison of L_∞ error norms in numerical solutions of Example 5.3 for $\Delta t = 0.001$.

t	L_∞(w)				CPU time (seconds)
	MQ quasi-interpolation technique (deg=9)($N = 50$)	MQ quasi-interpolation technique (deg=5)($N = 50$)	HWCM ($N = 32$)	Present Method ($N = 10$)	
0.05	0.0133	0.0135	7.808e-05	1.314e-07	3.4
0.10	0.0561	0.0568	1.336e-04	1.312e-07	4.6
0.15	0.1287	0.1392	1.920e-04	1.314e-07	6.1

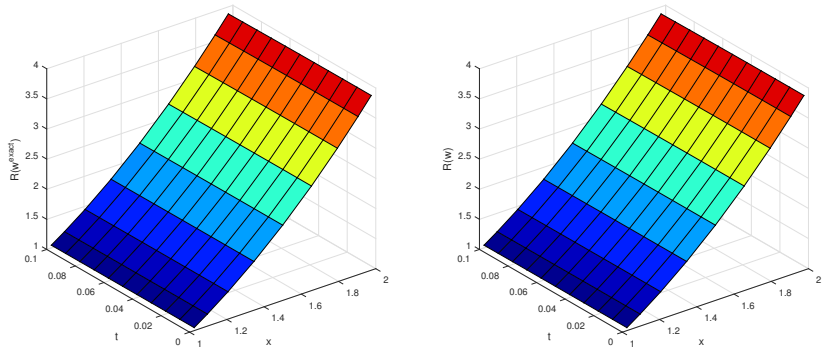

FIGURE 5. The real parts of exact and approximate solutions of Example 5.3 for $N = 10$.

The exact solution is given by

$$w(x,t) = x^2 e^{it}.$$

The numerical solutions of this example are presented in Table 6 and Figures 5-6 for the domain $[\alpha, \beta] = [1, 2]$. Table 6 shows CPU time for obtaining approximate solutions and comparison of maximum absolute error in solutions obtained by the present method and solutions obtained by MQ quasi-interpolation technique [14] and HWCM [3] for different values of t taking $\Delta t = 0.001$. It is observed that the present method provides a lesser error in comparison to MQ quasi-interpolation technique as well as HWCM for a smaller number of collocation points. The real and imaginary parts of the exact and approximate solutions of Example 5.3 are shown in Figures 5 and 6. It is revealed that the graphical representation of both exact and approximate solutions is the same.

Example 5.4. Consider nonlinear case of Equation (1.1) by taking $\phi = 1$, $\mu = -2$ and $\delta = 0$

$$iw_t + w_{xx} - 2|w|^2 w = 0,$$

subject to Dirichlet boundary conditions

$$w(\alpha, t) = e^{i(\alpha - 3t)}, \quad w(\beta, t) = e^{i(\beta - 3t)},$$

and initial condition

$$w(x, 0) = e^{ix}.$$

The exact solution is given by

$$w(x,t) = e^{i(x-3t)}.$$

The numerical results of Example 5.4 have been obtained for the domain $[\alpha, \beta] = [-1, 1]$ and are presented in tabular and graphical form. Table 7 depicts the comparative study of L_∞ error norms in approximate solutions at

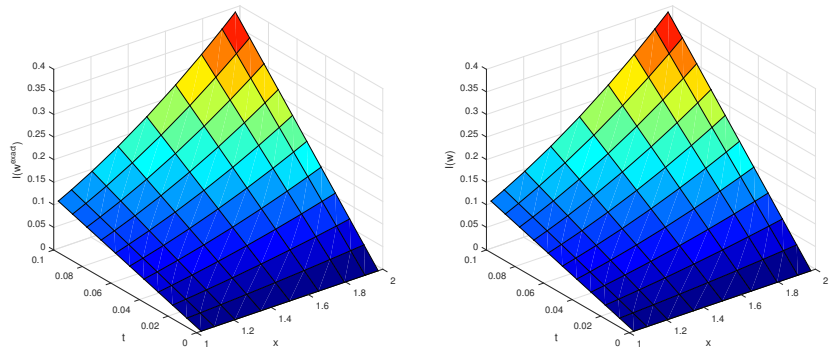

FIGURE 6. The imaginary parts of exact and approximate solutions of Example 5.3 for $N = 10$.

TABLE 7. Comparison of L_∞ error norms in approximate solutions of Example 5.4 at $t = 1$ taking $\Delta t = 0.001$.

N	J-GL-C method			Present method		
	$L_\infty(w)$	$L_\infty(R(w))$	$L_\infty(I(w))$	$L_\infty(w)$	$L_\infty(R(w))$	$L_\infty(I(w))$
2	2.43e-01	2.69e-01	3.23e-01	3.6365e-02	2.2695e-02	2.8414e-02
6	6.00e-05	5.68e-05	6.41e-05	4.0588e-06	1.4868e-06	4.0560e-06
10	2.26e-07	1.70e-07	2.35e-07	3.0109e-08	1.0951e-08	2.9838e-08

TABLE 8. L_∞ and L_2 error norms in approximate solutions of Example 5.4 taking $\Delta t = 0.001$ and $N = 10$.

t	$L_\infty(R(w))$	$L_\infty(I(w))$	$L_\infty(w)$	$L_2(R(w))$	$L_2(I(w))$	$L_2(w)$	CPU time (Seconds)
1	1.0951e-08	2.9838e-08	3.0109e-08	1.1994e-08	3.2966e-08	3.5080e-08	24.6
2	1.3344e-08	1.0141e-08	1.5384e-08	1.5942e-08	1.3037e-08	2.0593e-08	37.3
3	2.2416e-08	2.0384e-08	2.6434e-08	2.2822e-08	2.5273e-08	3.4053e-08	52.5
4	1.0007e-08	1.8217e-09	1.0007e-08	1.0267e-08	1.8407e-09	1.0431e-08	68.4
5	1.3471e-08	1.8294e-08	2.2437e-08	1.9140e-08	2.0376e-08	2.7956e-08	86.6

$t = 1$ obtained by the present method and J-GL-C method [13]. A better performance of the present method over J-GL-C method is observed from this table. Table 8 shows the error norms and CPU time in obtaining approximate solutions of Example 5.4 for different values of t taking $N = 10$. Further, Figures 7 and 8 depict the real and imaginary parts of the exact and approximate solutions of Example 5.4 in graphical form.

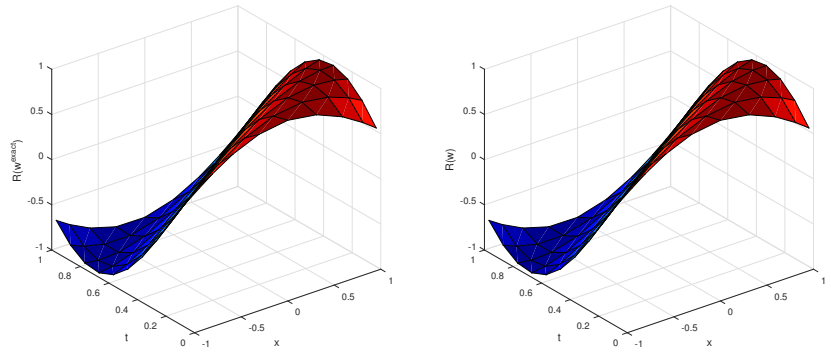

FIGURE 7. The real parts of exact and approximate solutions of Example 5.4 for $N = 10$.

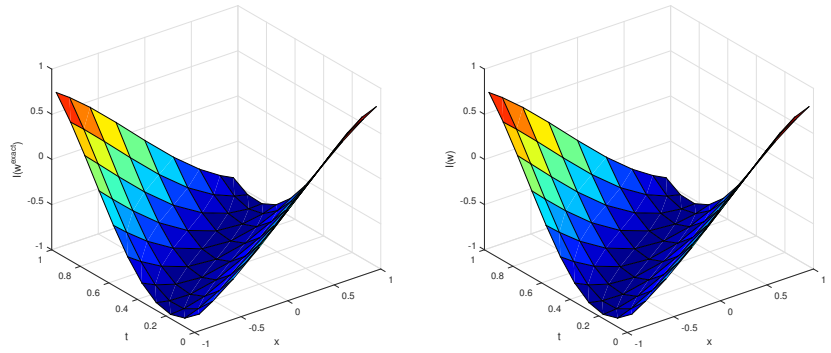

FIGURE 8. The imaginary parts of exact and approximate solutions of Example 5.4 for $N = 10$.

Example 5.5. Consider nonlinear case of Equation (1.1) by taking $\phi = 1, \mu = 2$ and $\delta = 0$

$$iw_t + w_{xx} + 2|w|^2 w = 0,$$

subject to Dirichlet boundary conditions

$$w(\alpha, t) = e^{i(\alpha+t)}, \quad w(\beta, t) = e^{i(\beta+t)},$$

and initial condition

$$w(x, 0) = e^{ix}.$$

The exact solution is $w(x, t) = e^{i(x+t)}$.

The approximate solutions of this problem have been obtained for two domains (i) $[\alpha, \beta] = [0, 1]$ and (ii) $[\alpha, \beta] = [-1, 1]$. Table 9 shows the error norms and CPU time for obtaining approximate solutions of Example 5.5 at $t = 1$ for $[\alpha, \beta] = [0, 1]$ taking $\Delta t = 0.001$. It is observed that the error norms decrease by increasing the value of N. The errors reduce to the order of 10^{-9} for $N = 8$. Table 10 depicts the comparison of L_∞ error norms in approximate solutions at $t = 1$ obtained by the present method and HWCM [3] for $[\alpha, \beta] = [0, 1]$. The comparison of L_∞ error norms in solutions given by the present method and J-GL-C method [13] is shown in Table 11 for $[\alpha, \beta] = [-1, 1]$. It is noticed from Tables 10 and 11 that the present method provides better accuracy as compared to HWCM and J-GL-C method

TABLE 9. L_∞ and L_2 error norms in approximate solutions of Example 5.5 at $t = 1$ for $\Delta t = 0.001$ and $x \in [0, 1]$.

N	$L_\infty(R(w))$	$L_\infty(I(w))$	$L_\infty(w)$	$L_2(R(w))$	$L_2(I(w))$	$L_2(w)$	CPU time (Seconds)
2	5.0248e-03	8.1526e-03	9.5768e-03	5.0248e-03	8.1526e-03	9.5768e-03	9.2
4	9.0064e-06	1.3131e-05	1.5795e-05	1.1362e-05	1.8464e-05	2.1680e-05	12.2
6	1.5133e-08	1.8654e-08	2.2919e-08	1.9804e-08	2.5456e-08	3.2252e-08	14.8
8	3.6382e-09	4.8847e-09	4.9943e-09	3.8265e-09	6.0714e-09	7.1766e-09	16.7

TABLE 10. Comparison of L_∞ error norms in approximate solutions of Example 5.5 at $t = 1$ for $\Delta t = 0.001$ and $x \in [0, 1]$.

Error norm	HWCM($N = 16$)	Present Method ($N = 8$)
$L_\infty(R(w))$	3.0944e-06	3.6382e-09
$L_\infty(I(w))$	3.3195e-05	4.8847e-09
$L_\infty(w)$	3.3318e-05	4.9943e-09

TABLE 11. Comparison of L_∞ error norms in approximate solutions of Example 5.5 at $t = 1$ for $\Delta t = 0.001$ and $x \in [-1, 1]$.

N	J-GL-C method			Present method		
	$L_\infty(w)$	$L_\infty(R(w))$	$L_\infty(I(w))$	$L_\infty(w)$	$L_\infty(R(w))$	$L_\infty(I(w))$
2	3.81e-01	5.73e-01	6.21e-01	1.4438e-01	8.9372e-02	1.1339e-01
6	3.62e-05	15.70e-05	16.04e-05	2.2721e-06	6.8194e-07	2.2451e-06
10	4.62e-08	22.59e-08	22.74e-08	2.2710e-09	9.7587e-10	2.1647e-09

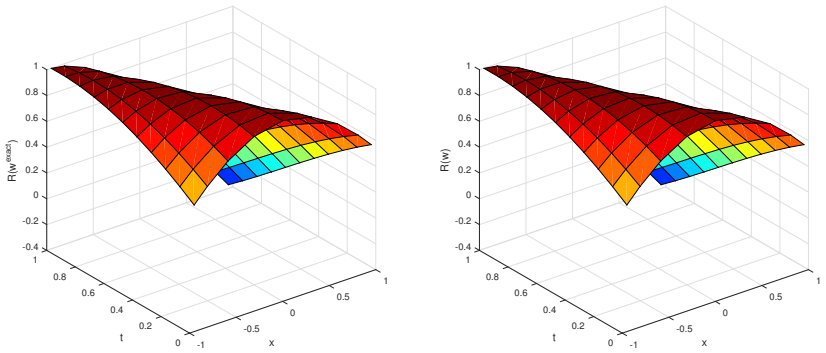

FIGURE 9. The real parts of exact and approximate solutions of Example 5.5 for $N = 10$.

for a small number of collocation points. In Figures 9 and 10, the real and imaginary parts of exact and approximate solutions for $[\alpha, \beta] = [-1, 1]$ have been shown graphically.

Example 5.6. Consider the nonlinear case of Equation (1.1)

$$iw_t + w_{xx} + 2|w|^2 w = 0,$$

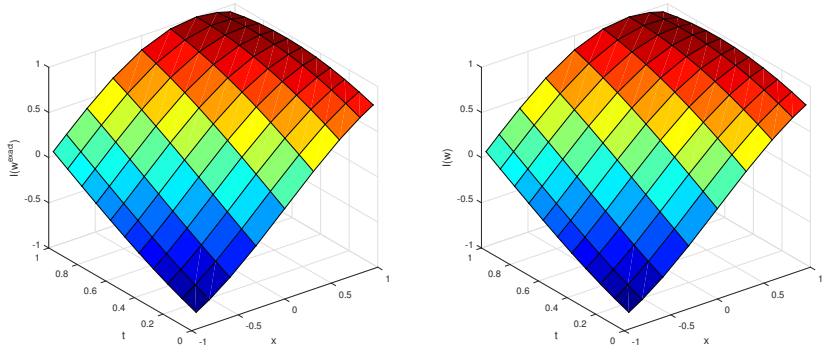

FIGURE 10. The imaginary parts of exact and approximate solutions of Example 5.5 for N=10.

TABLE 12. L_∞ and L_2 error norms in approximate solutions of Example 5.6 at $t = 1$ for $\Delta t = 0.001$ and $x \in [0, 1]$.

N	$L_\infty(R(w))$	$L_\infty(I(w))$	$L_\infty(w)$	$L_2(R(w))$	$L_2(I(w))$	$L_2(w)$	CPU time (Seconds)
2	3.7564e-01	1.7884e-01	4.1604e-01	3.7564e-01	1.7884e-01	4.1604e-01	8.0
4	7.7089e-03	4.7336e-03	8.8997e-03	9.5059e-03	6.4951e-03	1.1513e-02	10.5
6	4.0109e-05	3.2256e-05	4.2947e-05	5.4799e-05	4.5866e-05	7.1461e-05	14.2
8	1.3326e-07	8.7455e-07	8.8464e-07	2.2040e-07	1.5689e-06	1.5843e-06	16.0
10	2.5697e-08	7.7054e-08	7.8279e-08	3.2693e-08	9.1680e-08	9.7335e-08	19.5

subject to Dirichlet boundary conditions

$$w(\alpha, t) = e^{i(2\alpha-3t)} sech(\alpha - 4t), \quad w(\beta, t) = e^{i(2\beta-3t)} sech(\beta - 4t),$$

and initial condition

$$w(x, 0) = e^{2ix} sech(x).$$

The exact solution is given by

$$w(x, t) = e^{i(2x-3t)} sech(x - 4t).$$

The numerical solutions have been obtained for two domains (i) $[\alpha, \beta] = [0, 1]$ and (ii) $[\alpha, \beta] = [-1, 1]$. Table 12 presents the error norms and CPU time for obtaining approximate solutions of the nonlinear Schrödinger equation at $t = 1$ obtained by the present method taking $\Delta t = 0.001$ and different values of N for $[\alpha, \beta] = [0, 1]$. It is seen that error norms reduce to order 10^{-8} by increasing the value of N up to 10. Table 13 shows L_∞ error norms in approximate solutions of this example for $[\alpha, \beta] = [-1, 1]$. It is revealed that the L_∞ error norm is reduced to the order of 10^{-7} by fixing the value of $N = 15$. The real and imaginary parts of exact and approximate solutions for the domain $[\alpha, \beta] = [-1, 1]$ have been shown in Figures 11 and 12. A good agreement of exact and approximate solutions demonstrates the accuracy of the present method.

Example 5.7. Consider the nonlinear Schrödinger equation

$$iw_t + w_{xx} + |w|^2 w = 0,$$

TABLE 13. L_∞ error norms in approximate solutions of Example 5.6 at $t = 1$ for $\Delta t = 0.001$ and $x \in [-1, 1]$.

N	$L_\infty(w)$	$L_\infty(R(w))$	$L_\infty(I(w))$
2	6.5804e-01	5.3388e-01	3.8469e-01
5	4.0672e-02	4.0277e-02	2.9984e-02
10	4.4055e-05	4.4055e-05	2.3373e-05
15	1.5443e-07	3.8166e-08	1.4964e-07

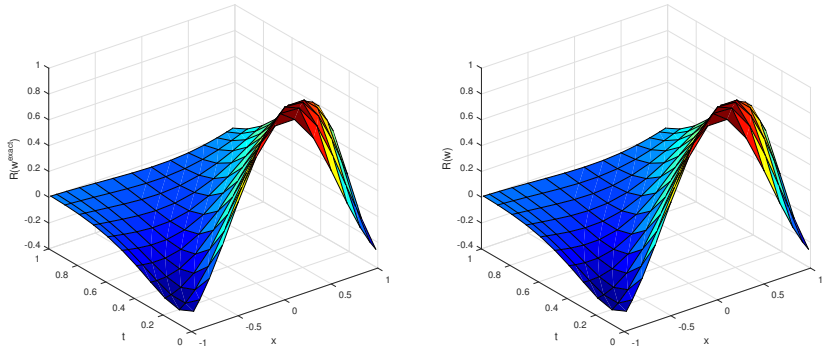

FIGURE 11. The real parts of exact and approximate solutions of Example 5.6 for $N = 15$.

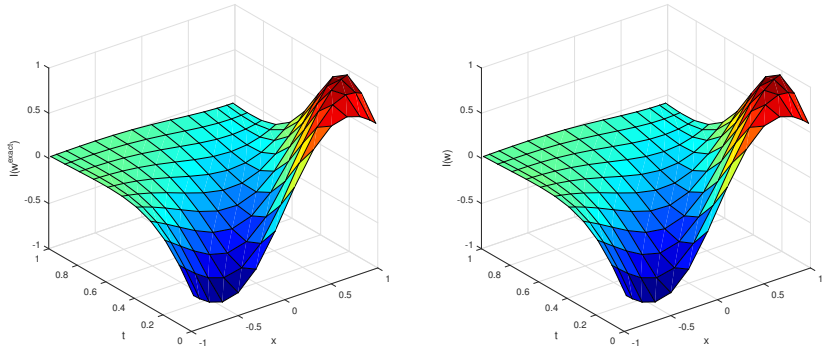

FIGURE 12. The imaginary parts of exact and approximate solutions of Example 5.6 for $N = 15$.

subject to Dirichlet boundary conditions

$$w(\alpha, t) = \sqrt{2}sech(\alpha - \frac{t}{2} + 10)exp(i(\frac{\alpha}{4} + \frac{15}{16}t)),$$
$$w(\beta, t) = \sqrt{2}sech(\beta - \frac{t}{2} + 10)exp(i(\frac{\beta}{4} + \frac{15}{16}t)),$$

and initial condition

$$w(x, 0) = \sqrt{2}sech(x + 10)exp(i(\frac{x}{4})).$$

TABLE 14. L_∞ and L_2 error norms in approximate solutions of Example 5.7 at $t = 1$ taking time steps $\Delta t = 0.001$ and 0.0001.

N	$\Delta t = 0.001$		CPU time	$\Delta t = 0.0001$		CPU time
	$L_\infty(w)$	$L_2(w)$	(seconds)	$L_\infty(w)$	$L_2(w)$	(seconds)
2	1.1025e-05	1.1025e-05	6.7	1.1025e-05	1.1025e-05	57.8
4	1.0084e-07	1.3285e-07	10.7	1.0084e-07	1.3285e-07	96.5
6	1.0097e-09	1.3034e-09	13.5	1.0097e-09	1.3034e-09	146.7
8	1.7699e-12	2.7323e-12	16.2	1.8438e-12	2.7804e-12	159.7
10	1.1849e-12	1.2880e-12	20.0	5.3663e-15	7.9392e-15	192.5

TABLE 15. L_∞ and L_2 error norms in approximate solutions of Example 5.7 at different time levels taking $N = 10$.

t	$\Delta t = 0.001$		$\Delta t = 0.0001$	
	$L_\infty(w)$	$L_2(w)$	$L_\infty(w)$	$L_2(w)$
0.1	3.9863e-13	5.5326e-13	2.6879e-15	4.3470e-15
0.2	6.0429e-13	8.0393e-13	4.3578e-15	6.3938e-15
0.3	5.5515e-13	6.2240e-13	3.2497e-15	5.0801e-15
0.4	2.6962e-13	3.3489e-13	1.8705e-15	3.1534e-15
0.5	5.0404e-13	7.2150e-13	2.9033e-15	4.4263e-15
0.6	8.5872e-13	9.9916e-13	4.3664e-15	6.3492e-15
0.7	8.4621e-13	8.7204e-13	4.1370e-15	5.9476e-15
0.8	5.8446e-13	7.0444e-13	2.1515e-15	3.5842e-15
0.9	8.0265e-13	1.0163e-12	3.6081e-15	5.8066e-15
1.0	1.1849e-12	1.2880e-12	5.3663e-15	7.9392e-15

The exact solution is given by

$$w(x,t) = \sqrt{2}sech(x - \frac{t}{2} + 10)exp(i(\frac{x}{4} + \frac{15}{16}t)).$$

The numerical solutions have been obtained for the domain $[\alpha, \beta] = [-1, 1]$. Table 14 shows the error norms and CPU time for obtaining approximate solutions of Example 5.7 at $t = 1$ by taking different values of time steps Δt and different values of N. Table 15 presents L_∞ error norms for approximate solutions obtained by the present method at different time levels for different values of Δt and fixed $N = 10$. Table 16 depicts the L_∞ and L_2 error norms in approximate solutions at different time levels taking $\Delta t = 0.0001$ for different values of N. From these tables, it is revealed that

(i) both error norms decrease by increasing the number of collocation points.
(ii) the error norms are smallest for $\Delta t = 0.0001$, and
(iii) the error norms reduce to the order of 10^{-15} for $\Delta t = 0.0001$ and $N = 10$.

Further, the real and imaginary parts of the exact and approximate solutions are depicted, respectively, in Figures 13 and 14 taking $\Delta t = 0.0001$.

6. Conclusion

In this paper, the shifted Chebyshev spectral collocation method is used for numerical solutions of linear and nonlinear Schrödinger equation with variable and constant coefficients. Chebyshev-Gauss-Lobatto points are used for collocation purposes and it is suggested that these collocation points produce accurate solutions. The convergence analysis of SCSCM has been demonstrated. The solutions of linear and nonlinear Schrödinger equations are complex-valued functions. The efficiency and accuracy of the present method have been demonstrated by considering seven

TABLE 16. L_∞ and L_2 error norms in approximate solutions of Example 5.7 for different time levels taking $\Delta t = 0.0001$.

t	$N = 6$		$N = 8$		$N = 10$	
	$L_\infty(w)$	$L_2(w)$	$L_\infty(w)$	$L_2(w)$	$L_\infty(w)$	$L_2(w)$
0.1	1.8546e-10	3.0088e-10	1.2953e-12	1.9258e-12	2.6879e-15	4.3470e-15
0.2	2.6290e-10	4.3322e-10	2.0594e-12	3.0396e-12	4.3578e-15	6.3938e-15
0.3	3.4843e-10	5.1375e-10	2.0423e-12	2.8884e-12	3.2497e-15	5.0801e-15
0.4	4.8900e-10	6.6416e-10	9.8641e-13	1.5826e-12	1.8705e-15	3.1534e-15
0.5	5.0087e-10	7.3941e-10	9.1615e-13	1.4128e-12	2.9033e-15	4.4263e-15
0.6	6.1828e-10	8.4164e-10	2.1631e-12	2.8741e-12	4.3664e-15	6.3492e-15
0.7	7.9609e-10	1.0329e-09	2.3369e-12	3.3321e-12	4.1370e-15	5.9476e-15
0.8	8.3520e-10	1.1465e-09	1.6773e-12	2.5562e-12	2.1515e-15	3.5842e-15
0.9	9.1567e-10	1.2267e-09	8.6802e-13	1.6811e-12	3.6081e-15	5.8066e-15
1.0	1.0097e-09	1.3034e-09	1.8438e-12	2.7804e-12	5.3663e-15	7.9392e-15

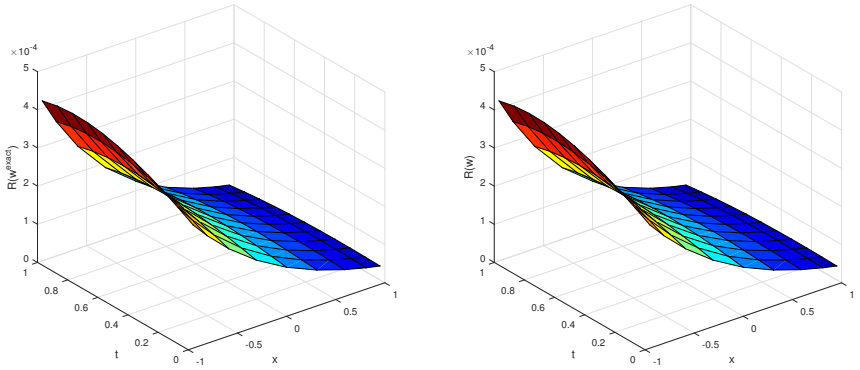

FIGURE 13. The real parts of exact and approximate solutions of Example 5.7 for $N = 10$ taking $\Delta t = 0.0001$.

examples of linear and nonlinear Schrödinger equations and presenting L_∞ and L_2 error norms in numerical solutions for different numbers of collocation points N. It is observed that error norms decrease by increasing the value of N and highly accurate solutions are obtained mostly for $N = 10$. Further, the error norms for the present method have been compared with error norms for other numerical methods such as HWCM, MQ quasi-interpolation technique and J-GL-C method. In comparison to these approaches, the present method provides better accuracy for a smaller number of collocation points. Thus, it consumes less processing time and computer memory for obtaining higher accuracies in numerical solutions. The approximate solutions of Example 5.7 have been obtained for two values of time step $\Delta t = 0.001$ and 0.0001. It is revealed that both the error norms are smaller for $\Delta t = 0.0001$ and they reduce to the order of 10^{-15} taking $N = 10$. Therefore, the present method is an efficient, accurate, effective and useful method to obtain the approximate solutions of linear and nonlinear Schrödinger equations. It will be helpful for the researchers and analysts who are engaged in numerical studies of modelling of different linear and nonlinear physical and engineering problems. The SCSCM can be extended for solving coupled and higher-dimensional linear and nonlinear Schrödinger equations.

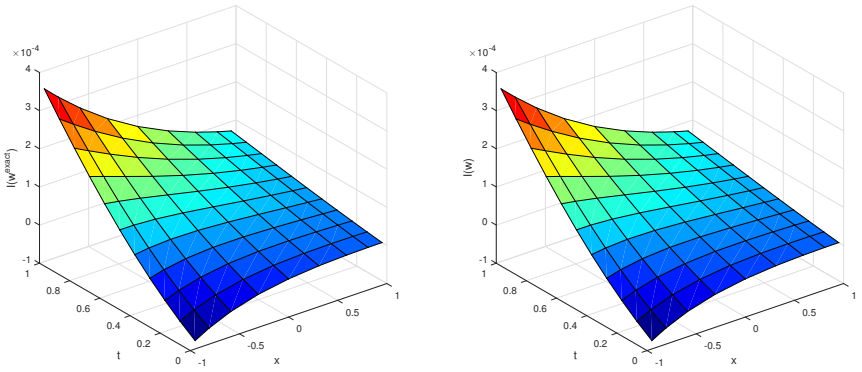

FIGURE 14. The imaginary parts of exact and approximate solutions of Example 5.7 for $N = 10$ taking $\Delta t = 0.0001$.

REFERENCES

[1] Y. E. Aghdam, H. Safdari, Y. Azari, H. Jafari, and D. Baleanu, *Numerical investigation of space fractional order diffusion equation by the Chebyshev collocation method of the fourth kind and compact finite difference scheme*, Discrete Contin. Dyn. Syst. S, *14*(7) (2021), 2025–2039.

[2] Y. E. Aghdam, H. Safdari, and M. Javidi, *Numerical approach of the space fractional order diffusion equation based on the third kind of Chebyshev polynomials*, In 4th International Conference on Combinatorics, Cryptography, Computer Science and Computing, (2019), 1231–1237.

[3] M. Ahsan, I. Ahmad, M. Ahmad, and I. Hussain, *A numerical Haar wavelet finite difference hybrid method for linear and non-linear Schrödinger equation*, Math. Comput. Simul., *169* (2019), 13–25.

[4] S. Ashrafi, M. Alineia, H. Kheiri, and G. Hojjati, *Spectral collocation method for the numerical solution of the Gardner and Huxley equations*, Int. J. Nonlinear Sci., *18* (2014), 71–77.

[5] Z. Avazzadeh, O. Nikan, and J. A. T. Machado, *Solitary wave solutions of the generalized Rosenau-KdV-RLW equation*, Mathematics., *8*(9) (2020), 1601.

[6] A. H. Bhrawy, *A Jacobi spectral collocation method for solving multi-dimensional nonlinear fractional sub-diffusion equations*, Numer. Algor., *73* (2016), 91–113.

[7] J. P. Boyd, *Chebyshev and Fourier spectral methods*, Dover Publications Inc, New York, 2000.

[8] C. Canuto, M. Y. Hussaini, A. Quarteroni, and T. A. Zang, *Spectral methods in fluid dynamics*, Springer-Verlag, Berlin Heidelberg, 1988.

[9] Q. Chang, E. Jia, and W. Sun, *Difference schemes for solving the generalized nonlinear Schrödinger equation*, J. Comput. Phys., *148*(2) (1999), 397–415.

[10] I. Dag, *A quadratic B-spline finite element method for solving nonlinear Schrödinger equation*, Comput. Methods Appl. Mech. Eng., *174*(1-2) (1999), 247-258.

[11] M. Dehghan and A. Taleei, *A Chebyshev Pseudospectral multidomain method for the soliton solution of the coupled nonlinear Schrödinger equations*, Comput. Phys. Commun., *182*(12) (2011), 2519–2529.

[12] M. Dehghan and A. Taleei, *Numerical solution of nonlinear Schrödinger equation by using time-space pseudo-spectral method*, Numer. Methods Partial Differ. Equ., *26*(4) (2010), 979–992.

[13] E. H. Doha, A. H. Bhrawy, M. A. Abdelkawy, and R. A. Van Gorder, *Jacobi-Gauss-Lobatto collocation method for the numerical solution of 1+1 nonlinear Schrödinger equations*, J. Comput. Phys., *261* (2014), 244–255.

[14] Y. Duan and F. Rong, *A numerical scheme for nonlinear Schrödinger equation by MQ quasi-interpolation*, Eng. Anal. Bound. Elem., *37*(1) (2013), 89–94.

[15] S. Jaiswal, M. Chopra, and S. Das, *Numerical solution of non-linear partial differential equation for porous media using operational matrices*, Math. Comput. Simul., *160* (2019), 138–154.
[16] A. Khan, M. Ahsan, E. Bonyah, R. Jan, M. Nisar, A. H. Abdel-Aty, and I.S. Yahia, *Numerical solution of Schrödinger equation by Crank-Nicolson method*, Math. Probl. Eng., *2022* (2022), 991067.
[17] A. H. Khater, R. S. Temsah, and M. M. Hassan, *A Chebyshev spectral collocation method for solving Burgers'-type equations*, J. Comput. Appl. Math., *222*(2) (2008), 333-350.
[18] H. Li and Y. Wang, *An averaged vector field Legendre spectral element method for the nonlinear Schrödinger equation*, Int. J. Comput. Math., *94*(6) (2017), 1196–1218.
[19] X. Liu, M. Ahsan, M. Ahmad, M. Nisar, X. Liu, I. Ahmad, and H. Ahmad, *Applications of Haar wavelet-finite difference hybrid method and its convergence for hyperbolic nonlinear Schrödinger equation with energy and mass conversion*, Energies., *14*(23) (2021), 7831.
[20] H. Mesgarani, A. Beiranvand, and Y. Esmaeelzade Aghdam, *The impact of the Chebyshev collocation method on solutions of the time-fractional Black-Scholes*, Math. Sci., *15* (2021), 137–143.
[21] O., Nikan and Z. Avazzadeh, *A locally stabilized radial basis function partition of unity technique for the sine–Gordon system in nonlinear optics*, Math. Comput. Simul., *199* (2022), 394–413.
[22] O. Nikan, Z. Avazzadeh, and M. N. Rasoulizadeh, *Soliton wave solutions of nonlinear mathematical models in elastic rods and bistable surfaces*, Eng. Anal. Bound. Elem., *143* (2022), 14–27.
[23] O. Oruc, A. Esen, and F. Bulut, *A Haar wavelet collocation method for coupled nonlinear Schrödinger–KdV equations*, Int. J. Mod. Phys. C., *27*(9) (2016), 1650103.
[24] N. Pervaiz and I. Aziz, *Haar wavelet approximation for the solution of cubic nonlinear Schrödinger equations*, Physica A: Stat. Mech. Appl., *545* (2020), 123738.
[25] M. N. Rasoulizadeh, Z. Avazzadeh, and O. Nikan, *Solitary wave propagation of the generalized Kuramoto-Sivashinsky equation in fragmented porous media*, Int. J. Appl. Comput. Math., *8* (2022), 252.
[26] M. P. Robinson, *The solution of nonlinear Schrödinger equations using orthogonal spline collocation*, Comput. Math. Appl., *33*(7) (1997), 39–57.
[27] H. Safdari, Y. E. Aghdam, and J. F. Gómez-Aguilar, *Shifted Chebyshev collocation of the fourth kind with convergence analysis for the space–time fractional advection-diffusion equation*, Eng. Comput., *38* (2022), 1409–1420.
[28] B. Saka, *A quintic B-spline finite element method for solving the nonlinear Schrödinger equation*, Phys. Wave Phenom., *20* (2012), 107–117.
[29] S. Sharma, U. S. Gupta, and R. Lal, *Effect of Pasternak foundation on axisymmetric vibration of polar orthotropic annular plates of varying thickness*, J. Vib. Acoust., *132*(4) (2010), 041001.
[30] Q. Sheng, A. Q. M. Khaliq, and E. A. Al-Said, *Solving the generalized nonlinear Schrödinger equation via quartic spline approximation*, J. Comput. Phys., *166*(2) (2001), 400–417.
[31] M. Smadi and D. Bahloul, *A compact split step Pade scheme for higher order nonlinear Schrödinger equation with power law nonlinearity and fourth order dispersion*, Comput. Phys. Commun., *182*(2) (2011), 366–371.
[32] M. A. Snyder, *Chebyshev Methods in Numerical Approximation*, Prentice-Hall, Inc., 1996.
[33] A. Taleei and M. Dehghan, *Time-splitting pseudo-spectral domain decomposition method for the soliton solutions of the one and multi-dimensional nonlinear Schrödinger equations*, Comput. Phys. Commun., *185*(6) (2014), 1515–1528.
[34] L. N. Trefethen, *Spectral Methods in Matlab*, SIAM, 2000.
[35] H. Wang, *Numerical studies on the split-step finite difference method for nonlinear Schrödinger equations*, Appl. Math. Comput., *170*(1) (2005), 17–35.
[36] Y. Wang, T. Wang, and G. H. Gao, *Series solution and Chebyshev collocation method for the initial value problem of Emden-Fowler equation*, Int. J. Comput. Math., *100*(2) (2023), 233–252.
[37] M. Zarebnia and S. Jalili, *Application of spectral collocation method to a class of nonlinear PDEs*, Commun. Numer. Anal., *2013* (2013), 1–14.
[38] H. Zhang, X. Jiang, C. Wang, and S. Chen, *Crank–Nicolson Fourier spectral methods for the space fractional nonlinear Schrödinger equation and its parameter estimation*. Int. J. Comput. Math., *96*(2) (2019), 238–263.